Supplementary materials for

Volumes and spin states of FeH_x: Implication for the density and temperature of the Earth's core

Hua Yang[1,2], Joshua M.R. Muir[1], Feiwu Zhang[1,*]

[1]State Key Laboratory of Ore Deposit Geochemistry, Institute of Geochemistry, Chinese Academy of Sciences, Guiyang, 550081, China

[2]University of Chinese Academy of Sciences, Beijing, 100049, China

*Corresponding author: F. Zhang (zhangfeiwu@vip.gyig.ac.cn)

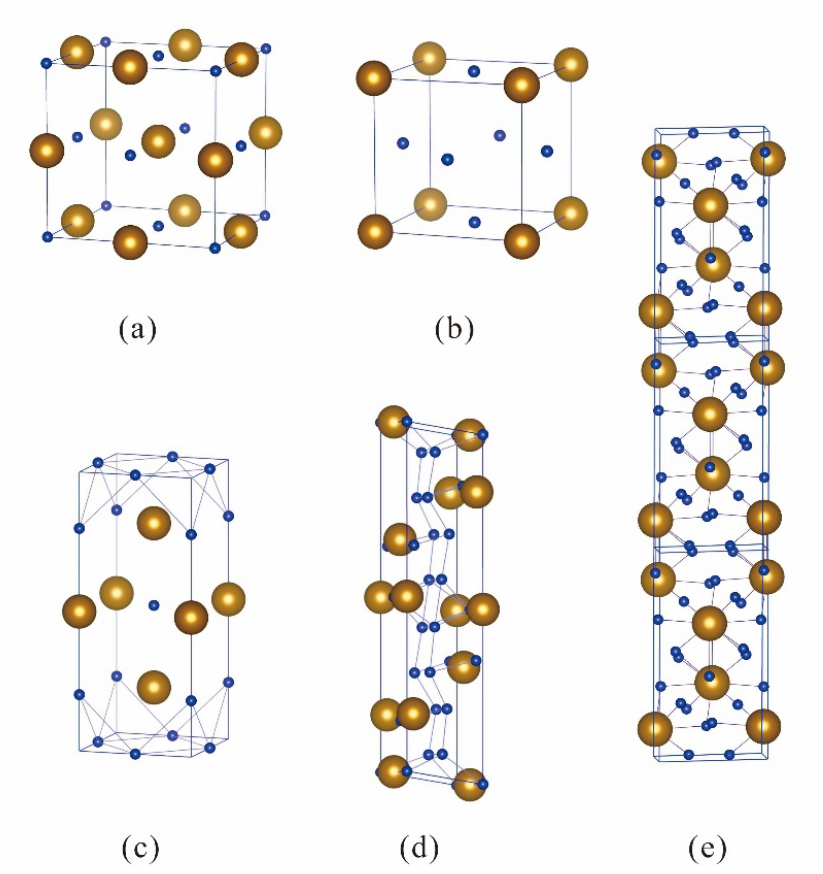

Figure S1. Crystal structures of iron hydrides compounds: (a) rocksalt-type FeH, (b) $Pm\bar{3}m$-FeH_3, (c) tetragonal structure of Fe_3H_5, (d) the C2/m phase of Fe_3H_{11}, and (e) C2/c phase of FeH_6. Large brown balls represent iron atoms, and small blue balls represent hydrogen atoms.

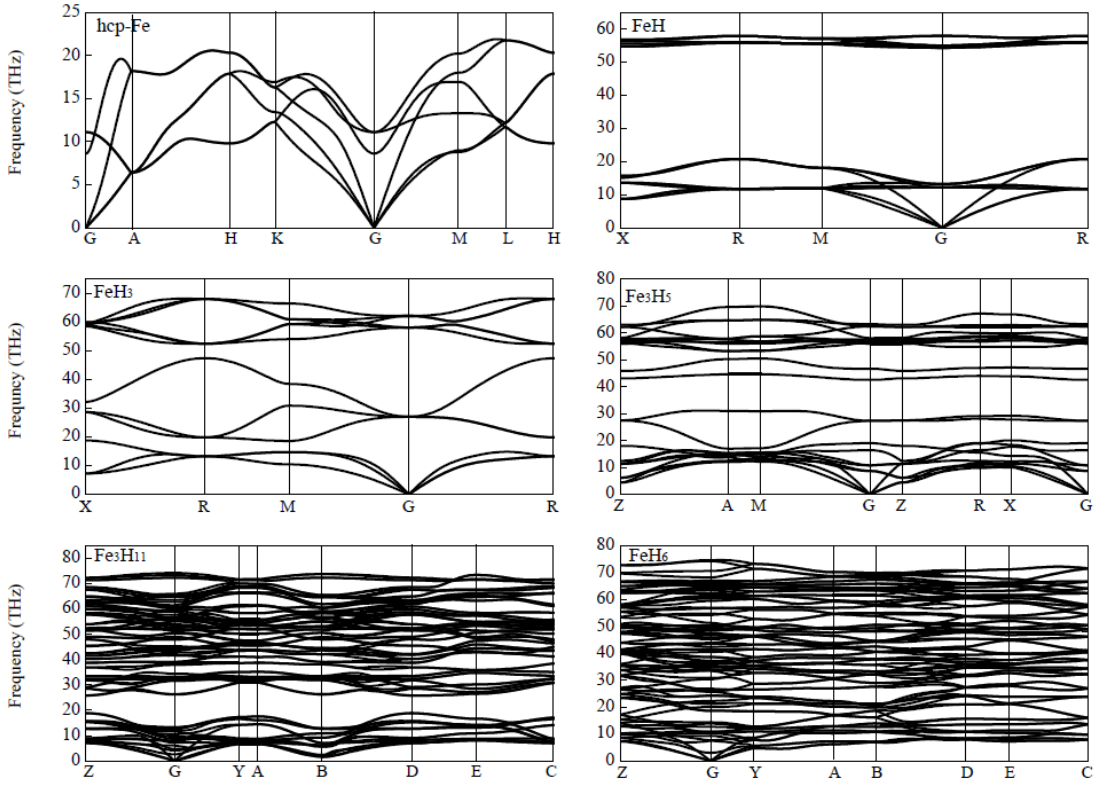

Figure S2. Calculated phonon dispersion curves of Fe-H phases at 360 GPa. All of the dispersion curves have no imaginary phonon frequencies, indicating that they are all dynamically stable.

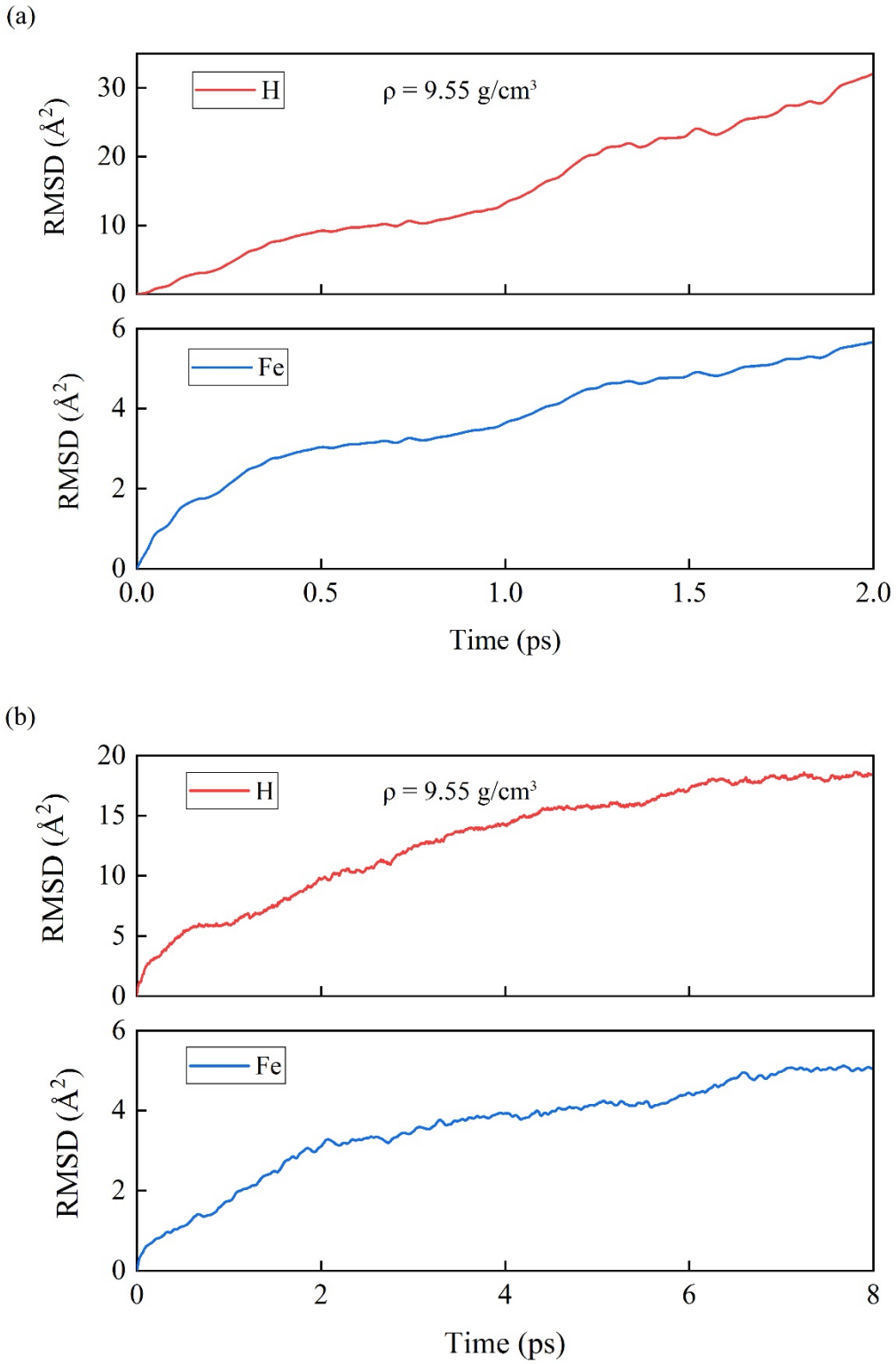

Figure S3. The root-mean-square displacement (RMSD) of H and Fe atoms in liquid *fcc*-$Fe_{32}H_{32}$ with densities of 9.55 g/cm^3. (a) melt at 10,000 K during 2 picoseconds (ps) and (b) equilibrate at 4000 K for 8 ps. The RMSD of H and Fe increase obviously with simulation time indicating a liquid state. The density corresponds to 135 GPa at 4000 K.

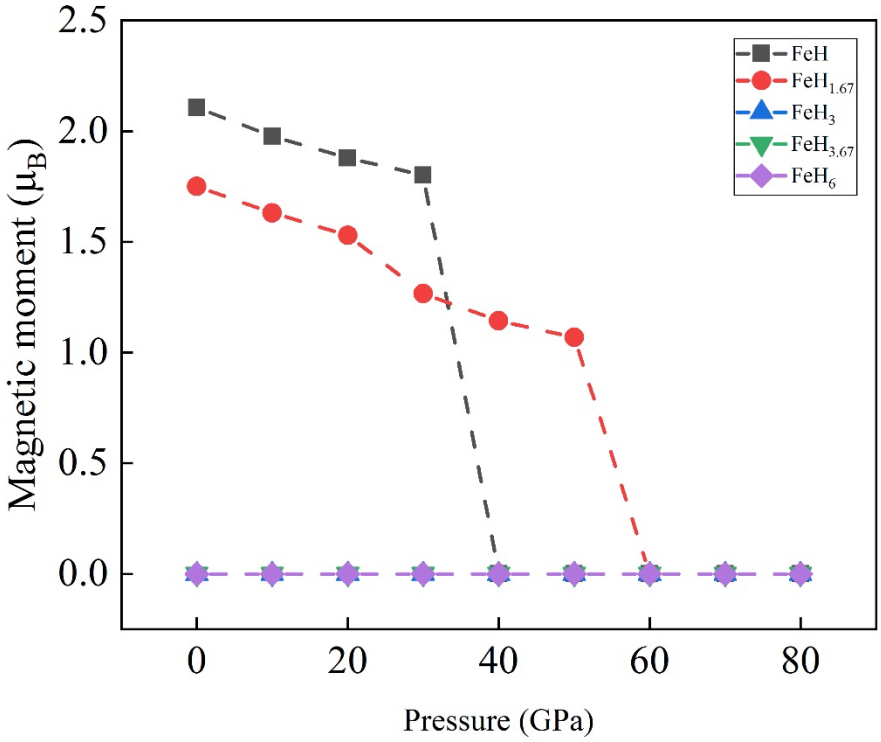

Figure S4. Magnetic moments per Fe atom of Fe-H binaries as a function of pressure. The magnetic moment collapses completely in the fcc FeH phase at a pressure of ~40 GPa (black squares). In Fe_3H_5 phase, the magnetic transition happens at a pressure of ~60 GPa (red circles). However, FeH_3, Fe_3H_{11}, and FeH_6 phases are always stable at the non-magnetic (NM) state. The dashed line is merely a guide to the eyes.

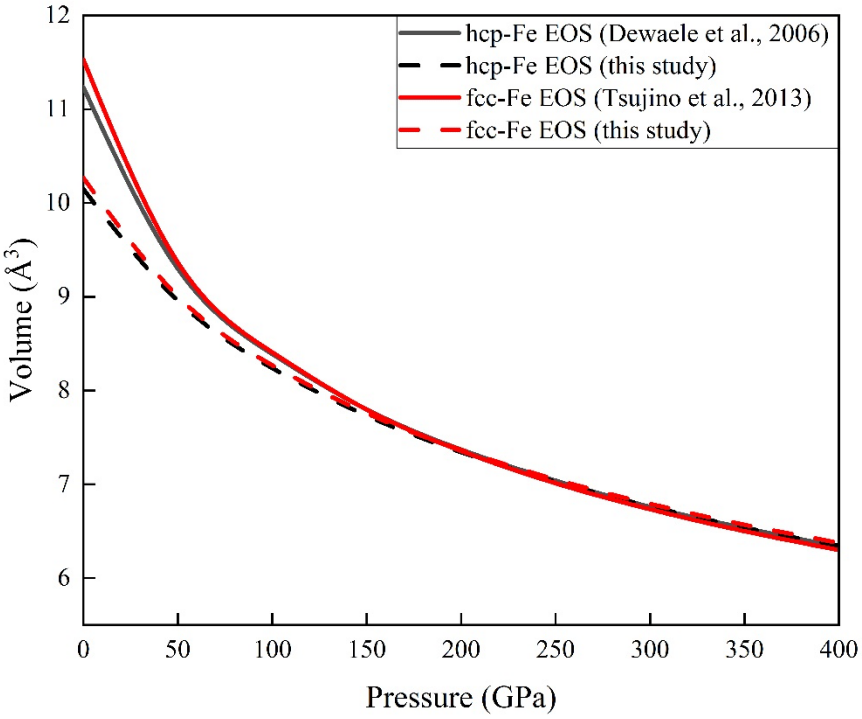

Figure S5. Equation of state (EOS) of pure hcp and fcc Fe at the pressure range of 0-400 GPa, where the experimental EOS of literature was also given for comparison. Above the pressure of ~200 GPa, the calculated EOS is well consistent with the experimental EOS. However theoretical absolute volumes suffer from small but non-negligible systematic errors of theory at low *P-T* conditions.

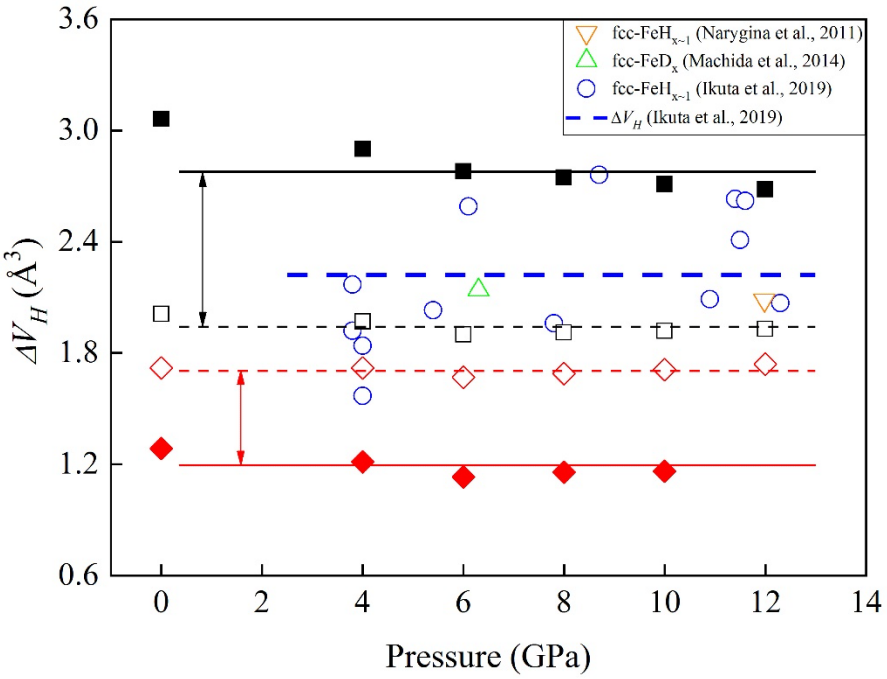

Figure S6. Hydrogen induced FeH volume expansion at low temperatures (<1200 K) and pressures (0-12 GPa). The black squares and red cubes are relative to the volume of hcp-Fe and fcc-Fe, respectively. Blue circles and the orange lower triangle are the experimental results determined by Ikuta et al. (2019) and Narygina et al. (2011), respectively. The green upper triangle is iron deuteride (FeD_x) at 6.3 GPa and 988 K determined by Machida et al. (2014). The dashed lines are the linear fit to the data points from the experiment, while the solid lines are the linear fit to the data points from the DFT calculations. Double arrows indicate errors between theoretical and experimental values.

Table S1. Predicted structures of the stable Fe-H binaries at 300 GPa.

Phases space group and lattice parameters	Wyckoff position	x	Y	z
Fe ($P6_3/mmc$) a = b = 2.149 Å, c = 3.389 Å	Fe 2d	0.667	0.333	0.25
FeH ($Fm\bar{3}m$) a = b = c = 3.156 Å	Fe 4b H 4a	0.00 0.00	0.50 0.50	0.00 0.50
FeH_3 ($Pm\bar{3}m$) a = b = c = 2.210 Å	Fe 4b H 4a	0.00 0.00	0.50 0.50	0.00 0.50
Fe_3H_5 (P 4/mmm) a = b = 2.227 Å, c = 5.347 Å	Fe 2h Fe 1b H 2g H 1d H 2f	0.50 0.00 0.00 0.50 0.00	0.50 0.00 0.00 0.50 0.50	0.206 0.50 0.202 0.50 0.00
FeH_6 (C 2/c) a = 3.525 Å, b = 5.973 Å, c = 3.158 Å β = 64.34°	H 8f H 8f H 4e H 4c Fe 4e	0.683 0.538 0.500 0.750 0.000	0.007 0.153 0.382 0.25 0.135	0.658 0.987 0.75 0.50 0.75
Fe_3H_{11} (C 2/m) a = 10.069 Å, b = 3.057 Å, c = 2.289 Å β = 80.64°	H 8j H 8j H 4i H 2a Fe 4i Fe 2b	0.570 0.298 0.35 0.50 0.333 0.50	0.261 0.206 0.00 0.50 0.50 0.00	0.454 0.627 0.092 0.00 0.082 0.00
H (Cmca) a = 2.559 Å, b = 4.751 Å, c = 2.865 Å	H 8f H 8f H 8f	0.50 0.50 0.00	0.868 0.732 0.004	1.454 1.361 0.635

Table S2. Theoretical third-order Birch-Murnaghan equation of state of the predicted Fe-H binaries.

Phase	$V_{0,}$ Å^3/f.u.	K_0, GPa	K_0'
P4/mmm-Fe_3H_5	42.32	242.83	4.14
Pm$\bar{3}$m-FeH_3	17.68	228.74	3.95
C2/m-Fe_3H_{11}	60.06	186.98	3.94
C2/c-FeH_6	28.56	131.33	3.92

Table S3. The probabilities (P_i) of different phases in relevant temperature at 300 GPa.

Probability	Phase	5000 K	6000 K
P_i	FeH	0.306	0.282
	Fe_3H_5	0.224	0.214
	FeH_3	0.117	0.111
	Fe_3H_{11}	0.215	0.233
	FeH_6	0.138	0.160

Note: The probability (P_i) of any specific arrangement is calculated by $P_i = \frac{1}{Z} e^{(-G_i/k_B T)}$, where $Z = \sum_i e^{(-G_i/k_B T)}$ and G_i is the Gibbs free energy of specific Fe-H binary.

Methods of calculating elastic properties:

The deformation matrix required to obtain the three non-zero elastic constants of the cubic phases (c11, c12, and c44) is given by:

$$\begin{pmatrix} 1+\delta & \delta/2 & 0 \\ \delta/2 & 1 & 0 \\ 0 & 0 & 1 \end{pmatrix}$$

The elastic moduli c_{ij} were evaluated using the stress-strain method by the standard relation $\sigma ij = c_{ijkl} \cdot \varepsilon_{kl}$. Four different strains (±0.01 and ±0.02) were applied in each distortion, and the resulting stress-strain values were then fitted to second-order polynomials. The seismic wave velocities were then obtained after computing the bulk elastic moduli and the shear elastic moduli in the Voigt average since we applied a uniform strain to the supercell (64 atoms); The Voigt average for the compressional modulus (K) of the cubic is given by:

$$K = \frac{C_{11} + 2C_{12}}{3}$$

While the shear modulus (G) of the cubic can be evaluated with:

$$G = \frac{C_{11} - C_{12} + 3C_{44}}{5}$$

And the compressional wave velocities V_p, shear wave velocities V_s, and bulk sound velocities V_ϕ can then be evaluated from the standard relations as follows:

$$V_p = \sqrt{\frac{K + \frac{4}{3}G}{\rho}}, \quad V_s = \sqrt{\frac{G}{\rho}}, \text{ and } V_\varphi = \sqrt{\frac{K}{\rho}}$$